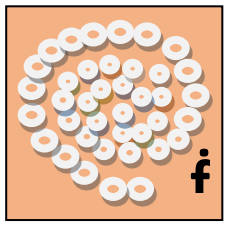

International Journal of Mathematical Analysis and Modelling

(Formerly Journal of the Nigerian Society for Mathematical Biology)

Volume 7 Issue 2, 2024

ISSN (Print): 2682 - 5694
ISSN (Online): 2682 – 5708
www.tnsmb.org

Characteristics and control strategies for Diphtheria-Pertussis co-infection risk in the post COVID-19 era

S.O. Johnson*†, H.O. Edogbanya †‡, J.O. Omolehin§, and O. Johnson¶

Abstract

Currently, the disruptions to routine vaccination programs induced during COVID-19 pandemic have raised worries about possible resurgence of vaccine-preventable diseases like diphtheria and pertussis, particularly in infants and children with zero vaccination. This study aims to assess the risk of diphtheria-pertussis co-dynamics and control strategies in the post-pandemic era using modified SIR-type mathematical model. Our research is hinged on the premise that pathogens can coexist in a host and that diphtheria-pertussis are both preventable by (Diphtheria-Tetanus-Pertussis) DTAP vaccine. Therefore, the presented model captures epidemiological parameters and varying disease control coverage inputs to simulate disease behaviour in a population susceptible to both infections. Key non-optimal control parameters used are vaccination at birth, maternal derived immunity and partial quarantine for diphtheria only. The next generation matrix was used to derive the basic reproduction number R_0 , after which stability analysis was conducted and it was observed that the formulated model exhibits four equilibrium points. The disease-free equilibrium and endemic equilibrium are shown to be locally and globally asymptotically stable. The forward sensitivity index was employed to pinpoint the effects of the hierarchy of parameters within R_0. Furthermore, it was observed that the model would undergo backward bifurcation under certain conditions, Consequently, optimal control inputs should be considered for future research. Finally, theoretical accuracy of the diseases co-existence is validated via Numerical simulations and relevant graphical illustrations are displayed using MATLAB 2021a.

Keywords and phrases: co-dynamics; effective reproduction number; sensitivity analysis; backward bifurcation; gaussian elimination

1 Introduction

The current trend in re-emergence of vaccine-preventable respiratory infectious diseases persist to be a global health concern with the increasing disruption on routine immunization by recent COVID-19 Pandemic [1, 2]. WHO and UNICEF Report available up to 2021 [3] estimated that about 25 million children missed out on DTP (Diphtheria-Tetanus-Pertussis) routine vaccines. According to [4], respiratory system disease affecting the lungs and other organs have long been a concern in children, pathogenic bacteria and virus that infect a human being can also be nested inside individual (host) itself. Hence, great importance is attributed to the characterization of co-infection by understanding how such pathogens intera t directly or indirectly through a carrier or its immigratory system [5, 6, 7, 8]. Diphtheria and pertussis are bacterial respiratory diseases with varying degrees of infection risk, both of which can be prevented by the DTaP (Diphtheria-Tetanus-Pertussis) vaccine [9, 10, 11]. Diphtheria, caused by the *Corynebacterium* species as noted by [12], can result in serious complications such

*Corresponding Author; E-mail: oladipuposamueljohnson@gmail.com
†Department of Mathematics, Federal University Lokoja, Kogi, Nigeria
‡E-mail: helen.edogbanya@fulokoja.edu.ng
§Department of Mathematics, Federal University Lokoja, Kogi, Nigeria; E-mail: joseph.omolehin@fulokoja.edu.ng
¶Department of Public Health, Ladoke Akintola University of Technology, Ogbomosho, Oyo, Nigeria; E-mail: olukunlelaiwola@gmail.com

as paralysis or death if the infection becomes chronic. The disease spreads through droplets or close contact with an infected individual, as the *bacterium Corynebacterium diphtheriae* releases a toxin that causes the illness. Pertussis, commonly known as whooping cough, is a highly contagious respiratory infection caused by the *bacterium Bordetella pertussis*. It spreads through droplets from an infected individual [13]. While severe pertussis can result in serious illness and even death, particularly in newborns and infants, the disease often goes undetected [14]. Research indicates that adolescents and adults, who may be asymptomatic carriers, are the primary source of infection for vulnerable infants. Recently, the co-interaction of pathogens has garnered significant attention from mathematicians worldwide. For example, [15] analyzed a co-dynamic model of pertussis-pneumonia, which includes a compartment for MDI (maternal-derived immunity) and temporary immunity among infected infants. Additionally, various studies have investigated the co-dynamic effects of pneumonia with other diseases, such as the HIV/AIDS-pneumonia co-infection dynamics studied by [16], and [17] examination of COVID-19 and bacterial pneumonia co-infection dynamics. In [18], a model was proposed for pneumonia-meningitis co-infection, while [19] studied influenza-meningitis co-infection, with a focus on quarantine and recovery rates. Additionally, [20] examined optimal control strategies for co-infections between chronic hepatitis B virus (HBV) and SARS-CoV-2, presenting a dynamic model that explores various equilibria and highlights the occurrence of backward bifurcation triggered by co-infection. The authors of [21, 22] utilized the Normalized Forward Sensitivity Index to assess the hierarchical influence of parameters on the reproduction number within the model. Furthermore, [22] investigated the potential coexistence of diphtheria and pertussis through mathematical modeling.

2 Model formulation

The diphtheria-pertussis co-infection model presented, comprises of eight different compartments, where, the total population at time (t) denoted as $N(t)$ is given by

$$N(t) = S(t) + I_{AD}(t) + I_{SD}(t) + I_{AP}(t) + I_{SP}(t) + I_{SDP}(t) + Q_{SD}(t) + R(t) \tag{1}$$

the compartments are Susceptible individuals $S(t)$, the infected individuals with diphtheria in asymptomatic stage $I_{AD}(t)$, the infected individuals with diphtheria in symptomatic stage $I_{SD}(t)$, the infected individuals with pertussis in asymptomatic stage $I_{AP}(t)$, the infected individuals with pertussis in symptomatic stage $I_{SP}(t)$, the infected individuals with both diphtheria and pertussis in there symptomatic stage $I_{SDP}(t)$, individuals who has recovered from diphtheria, pertussis or dual infection. $R(t)$, Quarantine of individuals showing clinical symptoms of diphtheria $Q_{SD}(t)$. In the model formulation, we assumed that $\kappa = bN(1-V)$ is the total proportion of zero vaccinated individuals where b is the birth rate and V is the vaccinated at birth. we also assume that due to vaccination during pregnancy, the mother would have passed on strong immunity to the infant via placenta at fetus stage. Therefore, the Susceptible or Vulnerable compartment S increases by the influx of non-vaccinated individuals and individuals who recovers from asymptomatic stage due to Maternal Derived Immunity (MDI) represented by $\xi_D I_{AD}$ and $\xi_P I_{AP}$ respectively.

Furthermore, The Susceptible compartment could get infected with diphtheria only at the rate $\Phi_D = \frac{\beta_D(\alpha_D I_{AD} + I_{SD})}{N}$, Pertussis only at rate $\Phi_P = \frac{\beta_P(\alpha_P I_{AP} + I_{SP})}{N}$, and dual infection at rate $\Phi_{DP} = \frac{\beta_{DP} I_{SDP}}{N}$ respectively. Individuals at the symptomatic stage of diphtheria and pertussis could get infected with a second infection at rates $\gamma_1 \frac{\beta_P(\alpha_P I_{AP} + I_{SP})}{N} I_{SD}$ and $\gamma_2 \frac{\beta_D(\alpha_D I_{AD} + I_{SD})}{N} I_{SP}$ respectively, where γ_1 and γ_2 denotes vulnerability to a second infection. We also assume that vaccinated individuals at birth are immune against disease and flows directly into the recovered compartment R at rate VbN. Other parameter used are described in Table 1

Based on the model description and assumptions above, we formulated the model governing equation (2).

Table 1: Values of parameters used in simulation.

Parameter	Symbol	Value	Cite
β_D	Effective contact rate for Diphtheria	0.57/day	[23]
β_P	Effective contact rate for Pertussis	0.5-1/day	[15]
β_{DP}	Diphtheria-Pertussis contact rate	0.2/day	fitted
ξ_D	MDI against Diphtheria infection	0.35	[15],
ξ_P	MDI against Pertussis	0.35	[15, 30]
ξ_{DP}	MDI Dual infection	0.35	[15]
Ω	Recovery rate of Quarantine	0.1-0.9	Assumed
η_D	Diphtheria Recovery rate.	0.5	[15]
η_P	Pertussis Recovery rate	$[\frac{1}{14}, 0.0206$	[15]
η_{DP}	Diphtheria-Pertussis Recovery rate	0.15/day	[19]
ϖ_D	Diphtheria induced death rate	0.05	[23]
ϖ_P	Pertussis induced death rate	0.0309	[15]
ϖ_{DP}	Disease induced death rate of Dual infection	0.005/day	[23]
μ	Natural death rate	0.006	[23]
θ	Diphtheria infected Quarantined	0.1/day	Assumed
V	Vaccination	0.1-1.2	Assumed
α_D, α_P	Modification parameter	0.5	[15]
γ_1, γ_2	Modification parameter	1	[19]
b	Birth rate	0.019	[23]
ϕ_D, ϕ_P	Progression to symptomatic infected stage	$[\frac{3}{7}]$/day , $[\frac{7}{7}]$/day	Fitted

$$
\begin{aligned}
\frac{dS}{dt}(t) &= bN(1-V) + \xi_D I_{AD} + \xi_P I_{AP} \\
&\quad - \left(\frac{\beta_D(\alpha_D I_{AD} + I_{SD})}{N} + \frac{\beta_P(\alpha_P I_{AP} + I_{SP})}{N} + \frac{\beta_{DP} I_{SDP}}{N} \right) S - \mu S \\
\frac{dI_{AD}}{dt}(t) &= \frac{\beta_D(\alpha_D I_{AD} + I_{SD})}{N} S - (\phi_D + \xi_D + \mu) I_{AD} \\
\frac{dI_{SD}}{dt}(t) &= \phi_D I_{AD} - (\theta + \eta_D + \varpi_D + \mu) I_{SD} - \gamma_1 \frac{\beta_P(\alpha_P I_{AP} + I_{SP})}{N} I_{SD} \\
\frac{dI_{AP}}{dt}(t) &= \frac{\beta_P(\alpha_P I_{AP} + I_{SP})}{N} S - (\phi_P + \xi_P + \mu) I_{AP} \\
\frac{dI_{SP}}{dt}(t) &= \phi_P I_{AP} - (\eta_P + \varpi_P + \mu) I_{SP} - \gamma_2 \frac{\beta_D(\alpha_D I_{AD} + I_{SD})}{N} I_{SP} \\
\frac{dI_{SDP}}{dt}(t) &= \frac{\beta_{DP} I_{SDP}}{N} S + \gamma_1 \frac{\beta_P(\alpha_P I_{AP} + I_{SP})}{N} I_{SD} + \gamma_2 \frac{\beta_D(\alpha_D I_{AD} + I_{SD})}{N} I_{SP} \\
&\quad - (\eta_{DP} + \varpi_{DP} + \mu) I_{SDP} \\
\frac{dQ_{SD}}{dt}(t) &= \theta I_{SD} - (\Omega + \mu) Q_{SD} \\
\frac{dR}{dt}(t) &= VbN + \eta_P I_{SP} + \eta_D I_{SD} + \eta_{DP} I_{SDP} + \Omega Q_{SD} - \mu R
\end{aligned}
\tag{2}
$$

$S(0) > 0, I_{AD}(0) > 0, I_{SD}(0) > 0, I_{AP}(0) > 0, I_{SP}(0) > 0, I_{SDP}(0) > 0, Q_{SD}(0) > 0$

Model Schematic Diagram is seen in Figure 1:

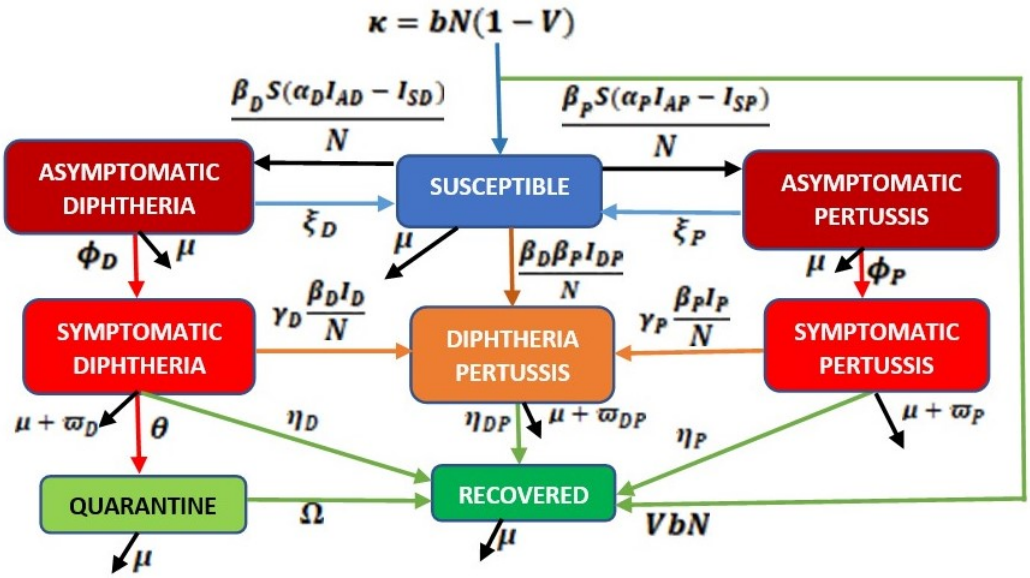

Figure 1: Schematic Diagram of Diphtheria-Pertussis transmission dynamics.

3 Analysis of the model

3.1 Model existence and uniqueness

To ensure that this diphtheria-pertussis transmission model is both mathematically and epidemiological sound, the dynamic system outlined in equation (2) must satisfy the subsequent theorems. We recall that the infection forces is $\Phi_D = \frac{\beta_D(\alpha_D I_{AD} + I_{SD})}{N}$, $\Phi_P = \frac{\beta_P(\alpha_P I_{AP} + I_{SP})}{N}$, and $\Phi_{DP} = \frac{\beta_{DP} I_{SDP}}{N}$ respectively which will subsequently be used interchangeably.

Theorem 1 (non-negativity or positively of model). If the initial value conditions for $S(0) > 0, I_{AD}(0) > 0, I_{SD}(0) > 0, I_{AP}(0) > 0, I_{SP}(0) > 0, I_{SDP}(0) > 0, R(0) > 0, Q_{SP}(0) > 0$ and $t(0) > 0 \ \forall \ t\epsilon[0, t_0]$ then, $S(t), I_{AD}(t), I_{SD}(t), I_{AP}(t), I_{SP}(t), I_{SDP}(t), R(t)$ and $Q_{SD}(t)$ Maintains positivity throughout in $\mathbb{R}^8_+$.

Proof. Giving that we are dealing with human populations, it is presupposed that all the employed parameter are non-negative. From equation (2), we assume that the Susceptible compartment is,

$$\frac{dS}{dt} = \kappa + \xi_D I_{AD} + \xi_P I_{AP} - (\Phi_D + \Phi_P + \Phi_{DP} + \mu)S \geq -(\Phi_D + \Phi_P + \Phi_{DP} + \mu)S \tag{3}$$

By separating variables in equation (3) and applying the integrating factor method, we derive

$$\frac{dS}{dt} \geq -(\Phi_D + \Phi_P + \Phi_{DP} + \mu)S \equiv \frac{dS}{S} \geq -(\Phi_D + \Phi_P + \Phi_{DP} + \mu)dt$$

$$\begin{aligned} \int_0^S \frac{dS}{S} &\geq -\int_0^t (\Phi_D + \Phi_P + \Phi_{DP} + \mu)dt \\ \ln|S(t)| &\geq -(\Phi_D + \Phi_P + \Phi_{DP} + \mu)t + C \\ S(t) &\geq Ce^{-(\Phi_D + \Phi_P + \Phi_{DP} + \mu)t} \end{aligned}$$

Hence, if $(t = 0)$ we have $(S(t) \geq S(0)e^{-(\Phi_D + \Phi_P + \Phi_{DP} + \mu)t} \geq 0)(\forall t > 0)$ since $(\Phi_D + \Phi_P + \Phi_{DP} + \mu) > 0$. Similarly, we can show that $(I_{AD}(t), I_{SD}(t), I_{AP}(t), I_{SP}(t), I_{SDP}(t), R(t))$ and $Q_{SD}(t)$ are non-negative.

Theorem 2 (Boundedness). The closed set given by $B^* = (S, I_{AD}, I_{SD}, I_{AP}, I_{SP}, I_{SDP}, R, Q_{SD}) \in \mathbb{R}^8_+ : S + I_{AD} + I_{SD} + I_{AP} + I_{SP} + I_{SDP} + R + Q_{SD} \leq \frac{\kappa}{\mu}\}$ is positively invariant with respect to the dynamic system equation (2).

Proof. Adding equation (2) and equating it to zero at initial time ($t = \varpi_D = \varpi_P = \varpi_{DP} = 0$) gives:

$$\frac{dN}{dt} + \mu N(t) \leq \kappa \tag{4}$$

Again, applying the integrating factor method to equation (4) and employing Gronwall's-Bellman inequality [21], followed by simplification, results in:

$$N(t) \leq \frac{\kappa}{\mu} + (N(0) - \frac{\kappa}{\mu})e^{-\mu t}, \Rightarrow N(t) \leq \frac{\kappa}{\mu}$$

As $t \to \infty$, the equation (2) has the solution in B^* and thus positively invariant.

Theorem 3 (Existence and uniqueness). Starting from the Initial values of the equation (2) , which are $S(0) > 0, I_{AD}(0) > 0, I_{SD}(0) > 0, I_{AP}(0) > 0, I_{SP}(0) > 0, I_{SDP}(0) > 0, R(0) > 0, Q_{SD}(0) > 0$, then $t \in \mathbb{R}$, the solutions $S(t)$, $I_{AD}(t)$, $I_{SD}(t)$, $I_{AP}(t)$, $I_{SP}(t)$, $I_{SDP}(t)$, $Q_{SD}(t)$, $R(t)$ exist in $\mathbb{R}^8_+$.

Proof. If the model equation (2) can be expressed in the form $\dot{x} = f(x)$ where,

$$\dot{x} = \begin{pmatrix} S \\ I_{AD} \\ I_{SD} \\ I_{AP} \\ I_{SP} \\ I_{SDP} \\ Q_{SD} \\ R \end{pmatrix}$$

$$f(x) = \begin{bmatrix} \kappa + \xi_D I_{AD} + \xi_P I_{AP} - (\Phi_D + \Phi_P + \Phi_{DP})\, S - \mu S \\ \Phi_D S - (\phi_D + \xi_D + \mu) I_{AD} \\ \phi_D I_{AD} - (\theta + \eta_D + \varpi_D + \mu) I_{SD} - \gamma_1 \Phi_P I_{SD} \\ \Phi_P S - (\phi_P + \xi_P + \mu) I_{AP} \\ \phi_P I_{AP} - (\eta_P + \varpi_P + \mu) I_{SP} - \gamma_2 \Phi_D I_{SP} \\ \Phi_{DP} S + \gamma_1 \Phi_P I_{SD} + \gamma_2 \Phi_D I_{SP} - (\eta_{DP} + \varpi_{DP} + \mu) I_{SDP} \\ \theta Q_{SD} - (\Omega + \mu) Q_{SD} \\ \eta_P I_{SD} + \eta_D I_{SP} + \eta_{SDP} I_{SDP} + \Omega Q_{SD} - \mu R \end{bmatrix} \tag{5}$$

Then equation (5) is proved by the existence and uniqueness theorem, since f has a continuous first derivative in $\mathbb{R}^8_+$ and is locally Lipschitz, therefore, there exists a unique, positive, and bounded solution for the governing equation (2) in $\mathbb{R}^8_+$.

3.1.1 Equilibrium solutions

Here, The equilibrium points is derived by equating all compartments in equation (2) to zero, i.e.,

$$\frac{dN}{dt} = \frac{dS}{dt} + \frac{dI_{AD}}{dt} + \frac{dI_{SD}}{dt} + \frac{dI_{AP}}{dt} + \frac{dI_{SP}}{dt} + \frac{dI_{SDP}}{dt} + \frac{dQ_{SD}}{dt} + \frac{dR}{dt} = 0$$

Upon diphtheria-pertussis initial outbreak which is the Disease Free Equilibrium we obtain:

$$\begin{aligned} N_0 &= (S_0 + I_{AD0} + I_{SD0} + I_{AP0} + I_{SP0} + I_{SDP0} + Q_{SD0} + R_0) \\ &= (\frac{\kappa}{\mu}, 0, 0, 0, 0, 0, 0, 0) \end{aligned}$$

Solving for the endemic Equilibria

In the absence of pertussis disease: $E_D^* = (S^*, I_{AD}^*, I_{SD}^*, 0, 0, 0, R^*)$ This account for the endemic equilibrium point of Diphtheria disease denoted as,

$$S^* = \frac{bN(1-V) + \xi_D I_{AD}^*}{\Phi_D^* + \mu}, I_{AD}^* = \frac{\beta_D I_{SD}^* S^*}{(\phi_D + \xi_D + \mu) - \beta_D \alpha_D},$$
$$I_{SD}^* = \frac{\phi_D I_{AD}^*}{(\theta + \eta_D + \varpi_D + \mu)}, R^* = \frac{VbN + \eta_D I_{SD}^*}{\mu}.$$

In the absence of Diphtheria disease: $E_P^* = (S^*, 0, 0, I_{AP}^*, I_{SP}^*, 0, R^*)$ This account for the endemic equilibrium point of pertussis disease, denoted as,

$$S^* = \frac{bN(1-V) + \xi_P I_{AP}^*}{\Phi_P^* + \mu}, I_{AP}^* = \frac{\beta_P I_{SP}^* S^*}{(\phi_P + \xi_P + \mu) - \beta_P \alpha_P},$$
$$I_{SP}^* = \frac{\phi_P I_{AP}^*}{(\theta + \eta_P + \varpi_P + \mu)}, R^* = \frac{VbN + \eta_P I_{AP}^*}{\mu}$$

In the presence of both diphtheria and pertussis co-infection state, $E_D^* = (S^*, I_{AD}^*, I_{SD}^*, I_{AP}^*, I_{SP}^*, I_{SDP}^*, R^*)$ This gives rise to the diphtheria-pertussis endemic equilibrium state given by.

$$S^* = \frac{bN(1-V) + \xi_D I_{AD}^* + \xi_P I_{AP}^*}{\Phi_D^* + \Phi_P^* + \Phi_{DP}^* + \mu}, I_{AD}^* = \frac{\beta_D I_{SD}^* S^*}{(\phi_D + \xi_D + \mu) - \beta_D \alpha_D},$$
$$I_{SD}^* = \frac{\phi_D I_{AD}^*}{(\theta + \eta_D + \varpi_D + \mu) + \gamma_1 \beta_P (\alpha_P I_{AP}^* + I_{SP}^*)},$$
$$I_{AP}^* = \frac{\beta_P I_{SP}^* S^*}{(\phi_P + \xi_P + \mu) - \beta_P \alpha_P}, I_{SP}^* = \frac{\phi_P I_{AP}^*}{(\eta_P + \varpi_P + \mu) + \gamma_1 \beta_D (\alpha_D I_{AD}^* + I_{SD}^*)},$$
$$I_{SDP}^* = \frac{\gamma_1 \beta_P (\alpha_P I_{AP}^* + I_{SP}^*) + \gamma_2 \beta_D (\alpha_D I_{AD}^* + I_{SD}^*)}{(\eta_{DP} + \xi_{DP} + \varpi_{DP} + \mu) - \beta_{DP}},$$
$$R^* = \frac{VbN + \eta_D I_{AD}^* + \eta_P I_{AP}^* + \eta_{DP} I_{SDP}^*}{\mu}$$

In a special case where the three infection forces are at steady state $\Phi_D^* = \frac{\beta_D I_{SD}^*}{N^*}$, $\Phi_P^* = \frac{\beta_P I_{SP}^*}{N^*}$, and $\Phi_{DP}^* = \frac{\beta_{DP} I_{SDP}^*}{N^*}$. The equation (2) possess co-existence endemic equilibria.

$$S^* = \frac{\kappa + \xi_D I_{AD}^* + \xi_P I_{AP}^*}{\Phi_D^* + \Phi_P^* + \Phi_{DP}^* + \mu}, I_{AD}^* = \frac{\Phi_D^* (\kappa + \xi_D I_{AD}^* + \xi_P I_{AP}^*)}{k_1 (\Phi_D^* + \Phi_P^* + \Phi_{DP}^* + \mu)},$$
$$I_{SD}^* = \frac{\alpha_D \Phi_D^* (\kappa + \xi_D I_{AD}^* + \xi_P I_{AP}^*)}{k_1 k_2 (\Phi_D^* + \Phi_P^* + \Phi_{DP}^* + \mu)}, I_{AP}^* = \frac{\Phi_P^* (\kappa + \xi_D I_{AD}^* + \xi_P I_{AP}^*)}{k_3 (\Phi_D^* + \Phi_P^* + \Phi_{DP}^* + \mu)},$$
$$I_{SP}^* = \frac{\alpha_P \Phi_P^* (\kappa + \xi_D I_{AD}^* + \xi_P I_{AP}^*)}{k_3 k_4 (\Phi_D^* + \Phi_P^* + \Phi_{DP}^* + \mu)}, I_{SDP}^* = \frac{\Phi_{DP}^* (\kappa + \xi_D I_{AD}^* + \xi_P I_{AP}^*)}{k_5 (\Phi_D^* + \Phi_P^* + \Phi_{DP}^* + \mu)},$$
$$R^* = \frac{(\kappa + \xi_D I_{AD}^* + \xi_P I_{AP}^*) (\Phi_D^* \eta_D \alpha_D k_3 k_4 k_5 + \Phi_P^* \eta_P \alpha_P k_1 k_2 k_5 + \Phi_{DP}^* \eta_{DP} k_1 k_2 k_3 k_4)}{\mu k_1 k_2 k_3 k_4 k_5 (\Phi_D^* + \Phi_P^* + \Phi_{DP}^* + \mu)}$$

3.2 Basic reproduction number

The Basic reproduction number R_0 which represents average number of secondary infections produced by an infected and infectious individual. Which implies that When $R_0 > 1$, the disease will persist within the population, particularly infants [24]. The next generation matrix is used to derive the basic reproduction number[24, 25] $R_0 = \rho F V^{-1}$, where ρ is the spectral radius and transition and transmission matrix are denoted by $F_i(a)$ and $V_i(a)$ at N_0 Respectively. Now let

$$k_1 = (\phi_D + \xi_D + \mu) I_{AD}, k_2 = (\theta + \eta_D + \varpi_D + \mu) I_{SD}, k_3 = (\phi_P + \xi_P + \mu) I_{AP},$$
$$k_4 = (\eta_P + \varpi_P + \mu) I_{SP}, k_5 = (\eta_{PD} + \varpi_{PD} + \mu) I_{SPD}.$$

$$FV^{-1} = \begin{bmatrix} \beta_D\alpha_D S & \beta_D S & 0 & 0 & 0 \\ 0 & 0 & 0 & 0 & 0 \\ 0 & 0 & \beta_P\alpha_P S & \beta_P S & 0 \\ 0 & 0 & 0 & 0 & 0 \\ 0 & 0 & 0 & 0 & \beta_{DP} S \end{bmatrix} \times \begin{bmatrix} \frac{1}{k_1} & 0 & 0 & 0 & 0 \\ \frac{\phi_D}{k_1 k_2} & \frac{1}{k_2} & 0 & 0 & 0 \\ 0 & 0 & \frac{1}{k_3} & 0 & 0 \\ 0 & 0 & \frac{\phi_P}{k_3 k_4} & \frac{1}{k_4} & 0 \\ 0 & 0 & 0 & 0 & \frac{1}{k_5} \end{bmatrix}$$

The Gaussian Elimination method was used to determine V^{-1} and dominant eigenvalue of FV^{-1} is given by

$$R_0 = \rho FV^{-1} = \max\{R_{0D}, R_{0P}, R_{0DP}\}$$

$$R_0 = \max\left\{\frac{b(1-v)}{\mu}\left(\frac{\beta_D(\alpha_D k_2 + \phi_D)}{k_1 k_2}, \frac{\beta_P(\alpha_P k_4 + \phi_P)}{k_3 k_4}, \frac{\beta_{DP}}{k_5}\right)\right\}$$

where, $S = \frac{\kappa}{\mu} = \frac{b(1-v)}{\mu}$

3.3 Stability analysis

The stability analysis of the disease free equilibrium point is carried out.

3.3.1 Local stability analysis of DFEP

Theorem 4 The diseases free equilibrium point is locally asymptomatic stable if $R_0 < 1$ and unstable if $R_0 > 1$, *Proof.* Jacobian matrix of the model equation (2) estimated at the disease-free equilibrium which yields

$$J_{dfe} = \begin{bmatrix} -\mu & -\beta_D\alpha_D & -\beta_D & \beta_P\alpha_P & -\beta_P & -\beta_{DP} & 0 \\ 0 & \beta_D\alpha_D - k_1 & \beta_D & 0 & 0 & 0 & 0 \\ 0 & \phi_D & -k_2 & 0 & 0 & 0 & 0 \\ 0 & 0 & 0 & \beta_P\alpha_P - k_3 & \beta_P & 0 & 0 \\ 0 & 0 & 0 & \phi_D & -k_4 & 0 & 0 \\ 0 & 0 & 0 & 0 & 0 & \beta_{DP} - k_5 & 0 \\ 0 & 0 & \eta_D & 0 & \eta_P & \eta_{SDP} & -\mu \end{bmatrix} \quad (6)$$

Then characteristic equation is expanded and determined using $|J_{dfe} - \lambda I| = 0$, where $\lambda_1 = 0$ twice and solutions of the equations is given by the remaining 2×2 , 1×1 sub-matrices below $R_{0D} k_1 k_2 = \beta_D(\alpha_D k_2 + \phi_D)$,

$$J_{dfe} = \begin{bmatrix} (\beta_D\alpha_D - k_1) - \lambda & \beta_D \\ \phi_D & -k_2 - \lambda \end{bmatrix} = \lambda^2 + (k_1 + k_2 - \beta_D\alpha_D)\lambda + k_1 k_2(1 - R_{0D}) = 0$$

$R_{0P} k_3 k_4 = \beta_P(\alpha_P k_4 + \phi_P)$,

$$J_{dfe} = \begin{bmatrix} (\beta_P\alpha_P - k_3) - \lambda & \beta_P \\ \phi_D & -k_4 - \lambda \end{bmatrix} = \lambda^2 + (k_3 + k_4 - \beta_P\alpha_P)\lambda + k_3 k_4(1 - R_{0P}) = 0$$

$(\beta_{DP} - k_5) - \lambda = \lambda + k_5(1 - R_{0DP})$

Thus, by Routh-hurwitz Stability criteria, all the roots of equation (6) have negative real parts $\Leftrightarrow$ $R_{0D} < 1$, $R_{0P} < 1$ and $R_{0DP} < 1$ Respectively. Therefore the disease free equilibrium is Asymptotic stable if $R_0 = \max\{R_{0D}, R_{0P}, R_{0DP}\} < 0$.

3.3.2 Global stability analyses of DFEP and EEP

In this section, we will use Lyapunov function method to show the global asymptotic stability of DFE and EEP by the following theorems

Theorem 5 The pertussis-free equilibrium is globally asymptotically stable $\Leftrightarrow R_0 \leq 1$.

Proof. to prove that the pertussis-free equilibrium is globally asymptotically stable, we will employ the Lyapunov function method by [27] . Now we will Consider a Lyapunov function candidate,

$$V_{AD} = \frac{I_{AD}}{\phi_D + \xi_D + \mu}$$

Taking the time derivative of V_{AD}:

$$\frac{dV_{AD}}{dt} = \frac{1}{\phi_D + \xi_D + \mu}\frac{dI_{AD}}{dt}$$

Substituting the value of $\frac{dI_{AD}}{dt}$:

$$\frac{dV_{AD}}{dt} = \frac{(\beta_D\alpha_D S - (\phi_D + \xi_D + \mu))I_{AD}}{\phi_D + \xi_D + \mu}$$

$$\Rightarrow \frac{dV_{AD}}{dt} = \frac{\beta_D\alpha_D S}{\phi_D + \xi_D + \mu}I_{AD} - I_{AD}$$

$$\Rightarrow \frac{dV_{AD}}{dt} \leq \left(\frac{\beta_D\alpha_D S}{\phi_D + \xi_D + \mu} - 1\right) I_{AD}$$

$$\Rightarrow \frac{dV_{AD}}{dt} \leq \left(\frac{b(1-V)\beta_D\alpha_D}{\mu(\phi_D + \xi_D + \mu)} - 1\right) I_{AD}$$

$$\frac{dV_{AD}}{dt} \leq (R_{0AD} - 1)I_{AD}$$

The above analysis shows that $\frac{dV_{AD}}{dt} \leq 0 \Leftrightarrow R_{0AD} \leq 1$ and also, $\frac{dV_{AD}}{dt} = 0 \Leftrightarrow I_{AD} = 0$ or R_{0AD} Thus, the pertussis-free equilibrium is globally asymptotically stable if $R_{0AD} \leq 1$.

Theorem 6 The diphtheria-free equilibrium is globally asymptotically stable $\Leftrightarrow R_{0AP} \leq 1$.

Proof. to prove that the diphtheria-free equilibrium is globally asymptotically stable, we will employ the Lyapunov function method by [27]. Now we will Consider a Lyapunov function candidate,

$$V_{AP} = \frac{I_{AP}}{\phi_P + \xi_P + \mu}$$

Taking the time derivative of V_{AP}:

$$\frac{dV_{AP}}{dt} = \frac{1}{\phi_P + \xi_P + \mu}\frac{dI_{AP}}{dt}$$

Substituting the value of $\frac{dI_{AP}}{dt}$:

$$\frac{dV_{AP}}{dt} = \frac{(\beta_P\alpha_P S - (\phi_P + \xi_P + \mu))I_{AP}}{\phi_P + \xi_P + \mu}$$

$$\Rightarrow \frac{dV_{AP}}{dt} = \frac{\beta_P\alpha_P S}{\phi_P + \xi_P + \mu}I_{AP} - I_{AP}$$

$$\Rightarrow \frac{dV_{AP}}{dt} \leq \left(\frac{\beta_P\alpha_P S}{\phi_P + \xi_P + \mu} - 1\right) I_{AP}$$

$$\Rightarrow \frac{dV_{AP}}{dt} \leq \left(\frac{b(1-V)\beta_P\alpha_P}{\mu(\phi_P+\xi_P+\mu)} - 1\right) I_{AP}$$

$$\frac{dV_{AP}}{dt} \leq (R_{0AP} - 1)I_{AP}$$

The above analysis shows that $\frac{dV_{AP}}{dt} \leq 0 \Leftrightarrow R_{0AP} \leq 1$ and also, $\frac{dV_{AP}}{dt} = 0 \Leftrightarrow I_{AP} = 0$ or R_{0AP} Thus, the pertussis-free equilibrium is globally asymptotically stable if $R_{0AP} \leq 1$.

Theorem 7 The co-infection endemic equilibrium of the basic model equation (2) is globally asymptotically stable.$\Leftrightarrow R_{0AP} \leq 1$

Proof. Using the common quadratic Lyapunov function method as in [27] and Considering a Lyapunov function candidate,

$$G(S, I_{AD}, I_{SD}, I_{AP}, I_{SP}, I_{SDP}, Q, R) =$$
$$\tfrac{1}{2}[(S - S^*) + (I_{AD} - I^*_{AD}) + (I_{SD} - I^*_{SD}) + (I_{AP} - I^*_{AP})$$
$$+(I_{SP} - I^*_{SP}) + (I_{SDP} - I^*_{SDP}) + (Q_{SD} - Q^*_{SD}) + (R - R^*)]^2$$

The time derivative of the Lyapunov function (G) is given by

$$\frac{dG}{dt} = [(S - S^*) + (I_{AD} - I^*_{AD}) + (I_{SD} - I^*_{SD}) + (I_{AP} - I^*_{AP})$$
$$+(I_{SP} - I^*_{SP}) + (I_{SDP} - I^*_{SDP}) + (Q_{SD} - Q^*_{SD}) + (R - R^*)][\tfrac{dS}{dt} + \tfrac{dI_{AD}}{dt}$$
$$+\tfrac{dI_{SD}}{dt} + \tfrac{dI_{AP}}{dt} + \tfrac{dI_{SP}}{dt} + \tfrac{dI_{SDP}}{dt} + \tfrac{dQ_{SD}}{dt} + \tfrac{dR}{dt}]$$

$$\frac{dG}{dt} = [(S - S^*) + (I_{AD} - I^*_{AD}) + (I_{SD} - I^*_{SD}) + (I_{AP} - I^*_{AP})$$
$$+(I_{SP} - I^*_{SP}) + (I_{SDP} - I^*_{SDP}) + (Q_{SD} - Q^*_{SD})$$
$$+(R - R^*)][\kappa - \mu(S + I_{AD} + I_{SD} + I_{AP} + I_{SP} + I_{SDP} + R + Q_{SD})]$$

given that

$$\kappa = \mu(S + I_{AD} + I_{SD} + I_{AP} + I_{SP} + I_{SDP} + R + Q_{SD})$$

$$\frac{dG}{dt} = [(S - S^*) + (I_{AD} - I^*_{AD}) + (I_{SD} - I^*_{SD}) + (I_{AP} - I^*_{AP})$$
$$+(I_{SP} - I^*_{SP}) + (I_{SDP} - I^*_{SDP}) + (Q - Q)^*)$$
$$+(R - R)^*][\kappa - \mu(S - S^*) + (I_{AD} - I^*_{AD}) + (I_{SD} - I^*_{SD}) + (I_{AP} - I^*_{AP})$$
$$+(I_{SP} - I^*_{SP}) + (I_{SDP} - I^*_{SDP}) + (Q - Q^*) + (R - R^*))]$$
$$= -\mu[(S - S^*) + (I_{AD} - I^*_{AD}) + (I_{SD} - I^*_{SD}) + (I_{AP} - I^*_{AP})$$
$$+(I_{SP} - I^*_{SP}) + (I_{SDP} - I^*_{SDP}) + (Q_{SD} - Q^*_{SD}) + (R - R^*))]^2 \leq 0$$

Here, $\frac{dG}{dt} \leq 0$ Note also that $\frac{dG}{dt} = 0 \Leftrightarrow S = S^*, I_{AD} = I^*_{AD}, I_{SD} = I^*_{SD}, I_{AP} = I^*_{AP}, I_{SP} = I^*_{SP}, I_{SDP} = I^*_{SDP}, Q_{SD} - Q^*_{SD}, R - R^*$. It is seen that by the common quadratic Lyapunov method, the co-infection endemic equilibrium is globally asymptotically stable.

3.3.3 Backward bifurcation analysis

ver time, several researchers globally has accepted that reducing the reproduction number to less than one infectious person $R_0 < 1$ is necessary and sufficient to eradicate a disease. However, in recent times this perspective has been challenged by several mathematicians globally and to this effect, numerous theoretical studies has been done to show that this criterion might not always be enough or adequate. The backward bifurcation phenomenon provides an alternative explanation, since it demonstrates that under certain conditions, even when the Disease-Free Equilibrium is stable and the reproduction number is less than unity $R_0 < 1$, At that point, there might exist a stable endemic equilibrium coexisting simultaneously.

Our aim in this section is to adopt the Castillo Chavez and Song approach [28] to show the existence of backward bifurcation at $R = 1$. Now, replacing the state variables as shown bellow;

$$S = x_1, I_{AD} = x_2, I_{SD} = x_3, I_{AP} = x_4, I_{SP} = x_5, I_{SDP} = x_6, Q_{SD} = x_7, R = x_8$$

so that the total population becomes

$$N = x_1 + x_2 + x_3 + x_4 + x_5 + x_6 + x_7 + x_8$$

Then, equation (2) takes on the new form

$$\begin{aligned}
\frac{dx_1}{dt}(t) &\equiv f_1 = bN(1-V) + \xi_D x_2 + \xi_P x_4 \\
&\quad - \left(\frac{\beta_D(\alpha_D x_2 + x_3)}{N} + \frac{\beta_P(\alpha_P x_4 + x_5)}{N} + \frac{\beta_{DP} x_6}{N} \right) x_1 - \mu x_1 \\
\frac{dx_2}{dt}(t) &\equiv f_2 = \frac{\beta_D(\alpha_D x_2 + x_3)}{N} x_1 - (\phi_D + \xi_D + \mu) x_2 \\
\frac{dx_3}{dt}(t) &\equiv f_3 = \phi_D x_2 - (\theta + \eta_D + \varpi_D + \mu) x_3 - \gamma_1 \frac{\beta_P(\alpha_P x_4 + x_5)}{N} x_3 \\
\frac{dx_4}{dt}(t) &\equiv f_4 = \frac{\beta_P(\alpha_P x_4 + x_5)}{N} x_1 - (\phi_P + \xi_P + \mu) x_4 \\
\frac{dx_5}{dt}(t) &\equiv f_5 = \phi_P x_4 - (\eta_P + \varpi_P + \mu) x_5 - \gamma_2 \frac{\beta_D(\alpha_D x_2 + x_3)}{N} x_5 \\
\frac{dx_6}{dt}(t) &\equiv f_6 = \frac{\beta_{DP} x_6}{N} x_1 + \gamma_1 \frac{\beta_P(\alpha_P x_4 + x_5)}{N} x_3 \\
&\quad + \gamma_2 \frac{\beta_D(\alpha_D x_2 + x_3)}{N} x_5 - (\eta_{DP} + \xi_{DP} + \varpi_{DP} + \mu) x_6 \\
\frac{dx_7}{dt}(t) &\equiv f_7 = VbN + \eta_P I_{SP} + \eta_D x_3 + \eta_{DP} x_6 - \mu x_7
\end{aligned} \tag{7}$$

where,

$$N = \sum_{i=1}^{7} x_i$$

now lets consider a special case when the reproduction number $R_0 = max\{R_{0D}, R_{0P}, R_{0DP}\} = 1$ Also, we suppose that $\beta_D = \beta_D^*$ be chosen as a bifurcation coefficient. from $R_{0D} = 1$, then equation becomes

$$\Rightarrow \quad 1 = \frac{\beta_D(\alpha_D k_2 + \phi_D)}{k_1 k_2} \Rightarrow \quad \beta_D = \beta_D^* = \frac{k_1 k_2}{\alpha_D k_2 + \phi_D}$$

Now, taking the Jacobian matrix of the system of equations at the disease free equilibrium point E_{0D}, denoted by $J(E_{0D})$, which yields

$$J(E_{0D}) = \begin{bmatrix}
-\mu & -\beta_D\alpha_D & -\beta_D & -\beta_P\alpha_P & -\beta_P & 0 & 0 \\
0 & \beta_D\alpha_D - k_1 & \beta_D & 0 & 0 & 0 & 0 \\
0 & \phi_D & -k_2 & 0 & 0 & 0 & 0 \\
0 & 0 & 0 & \beta_P\alpha_P - k_3 & \beta_P & 0 & 0 \\
0 & 0 & 0 & \phi_D & -k_4 & 0 & 0 \\
0 & 0 & 0 & 0 & 0 & -k_5 & 0 \\
0 & 0 & \eta_D & 0 & \eta_P & \eta_{DP} & -\mu
\end{bmatrix}$$

before employing the assumptions in theorem 4.1 of [28], it is vital to note the two types of eigenvectors of the matrix $J(E_{0D})$ for the case $R_{0D} = 1$ of the system equation (7) at the selected $\beta_D = \beta_D^*$ which are the right and left eigenvectors linked with the zero eigenvalues of $J(E_{0D})$. given by $\psi = (\psi_1, \psi_2, \psi_3, \psi_4, \psi_5, \psi_6, \psi_7)^T$ are determined as

$$J(E_{0D}) \cdot \psi = 0$$

implies

$$\begin{bmatrix} -\mu & -\beta_D\alpha_D & -\beta_D & -\beta_P\alpha_P & -\beta_P & 0 & 0 \\ 0 & \beta_D\alpha_D - k_1 & \beta_D & 0 & 0 & 0 & 0 \\ 0 & \phi_D & -k_2 & 0 & 0 & 0 & 0 \\ 0 & 0 & 0 & \beta_P\alpha_P - k_3 & \beta_P & 0 & 0 \\ 0 & 0 & 0 & \phi_P & -k_4 & 0 & 0 \\ 0 & 0 & 0 & 0 & 0 & -k_5 & 0 \\ 0 & 0 & \eta_D & 0 & \eta_P & \eta_{DP} & -\mu \end{bmatrix} \times \begin{bmatrix} \psi_1 \\ \psi_2 \\ \psi_3 \\ \psi_4 \\ \psi_5 \\ \psi_6 \\ \psi_7 \end{bmatrix} = \begin{bmatrix} 0 \\ 0 \\ 0 \\ 0 \\ 0 \\ 0 \\ 0 \end{bmatrix}$$

$\Rightarrow$

In order to observe assumptions 2 in theorem 4.1 of [28], that is making the right eigenvector non-negative from the third equation, solving ψ_3 in terms of ψ_2 gives

$$\psi_3 = \frac{\phi_D\psi_2}{k_2}$$

Substituting ψ_3 above into the second equation $(\beta_D\alpha_D - k_1)\psi_2 + \beta_D\psi_3 = 0 \Rightarrow$

$$\psi_2 = (\beta_D\alpha_D - k_1)\psi_2 + \frac{\beta_D\phi_D\psi_2}{k_2} = (\beta_D\alpha_D - k_1 + \frac{\beta_D\phi_D}{k_2})\psi_2 = 0$$

for $\psi_2 \neq 0$, means that ψ_2 coefficient $(\beta_D\alpha_D - k_1 + \frac{\beta_D\phi_D}{k_2}) = 0$, so that $k_1 = (\beta_D\alpha_D + \frac{\beta_D\phi_D}{k_2})$. Now, in a non-trivial sense, we can say $\psi_2 = \psi_2 > 0$ since it does not necessarily make ψ_2 tend to zero. Therefore, in same vein, $\psi_3 = \frac{\phi_D\psi_2}{k_2} > 0$, $\psi_4 = \psi_4 > 0$, $\psi_5 = \frac{\phi_D\psi_4}{k_4} > 0, \psi_6 = 0$,

$$\nu \cdot J(E_{0D}) = 0$$

implies

$$\begin{bmatrix} \nu_1 \\ \nu_2 \\ \nu_3 \\ \nu_4 \\ \nu_5 \\ \nu_6 \\ \nu_7 \end{bmatrix}^T \times \begin{bmatrix} -\mu & -\beta_D\alpha_D & -\beta_D & -\beta_P\alpha_P & -\beta_P & 0 & 0 \\ 0 & \beta_D\alpha_D - k_1 & \beta_D & 0 & 0 & 0 & 0 \\ 0 & \phi_D & -k_2 & 0 & 0 & 0 & 0 \\ 0 & 0 & 0 & \beta_P\alpha_P - k_3 & \beta_P & 0 & 0 \\ 0 & 0 & 0 & \phi_P & -k_4 & 0 & 0 \\ 0 & 0 & 0 & 0 & 0 & -k_5 & 0 \\ 0 & 0 & \eta_D & 0 & \eta_P & \eta_{DP} & -\mu \end{bmatrix} = \begin{bmatrix} 0 \\ 0 \\ 0 \\ 0 \\ 0 \\ 0 \\ 0 \end{bmatrix}$$

Similarly, the left eigenvectors components of $J(E_{0D})|_{\beta=\beta^*}$, $\nu = (\nu_1, \nu_2, \nu_3, \nu_4, \nu_5, \nu_6, \nu_7)$ satisfying $\psi \cdot \nu = 1$ are: $\nu_2 = \nu_2 > 0$, $\nu_3 = \frac{\beta_D\nu_2}{k_2} > 0$, $\nu_4 = \nu_4 > 0$, $\nu_5 = \frac{\beta_P\nu_4}{k_4} > 0$, $\nu_6 = 0$,
Considering assumption 1 and 2 earlier cited in theorem 4.1 of [28], the sign of a and b in the equations below ensures whether the model undergoes forward or backward bifurcation.

$$a = \sum_{i,j,k=1}^{7} \nu_i\psi_j\psi_k \frac{\partial^2 f_i}{\partial x_j \partial x_k}(0,0) \quad \text{and} \quad b = \sum_{i,j,k=1}^{7} \nu_i\psi_j \frac{\partial^2 f_i}{\partial x_j \partial \beta_D^*}(0,0)$$

$$a = \nu_2 \sum_{i,j,k=1}^{7} \psi_j\psi_k \frac{\partial^2 f_1}{\partial x_j \partial x_k} + \nu_4 \sum_{i,j,k=1}^{7} \psi_j\psi_k \frac{\partial^2 f_1}{\partial x_j \partial x_k}$$

$$\frac{\partial^2 f_2}{\partial x_1 \partial x_2} = \frac{\partial^2 f_2}{\partial x_2 \partial x_1} = -\frac{\beta_D \alpha_D}{N}, \quad \frac{\partial^2 f_2}{\partial x_1 \partial x_3} = \frac{\partial^2 f_2}{\partial x_3 \partial x_1} = -\frac{\beta_D}{N},$$
$$\frac{\partial^2 f_4}{\partial x_1 \partial x_4} = \frac{\partial^2 f_4}{\partial x_4 \partial x_1} = -\frac{\beta_P \alpha_P}{N}, \quad \frac{\partial^2 f_4}{\partial x_1 \partial x_5} = \frac{\partial^2 f_4}{\partial x_5 \partial x_1} = -\frac{\beta_P}{N},$$
$$\frac{\partial^2 f_6}{\partial x_1 \partial x_6} = \frac{\partial^2 f_6}{\partial x_6 \partial x_1} = -\frac{\beta_{DP}}{N}, \quad \frac{\partial^2 f_3}{\partial x_3 \partial x_4} = \frac{\partial^2 f_3}{\partial x_4 \partial x_3} = -\gamma_1 \frac{\beta_P \alpha_P}{N},$$
$$\frac{\partial^2 f_3}{\partial x_3 \partial x_5} = \frac{\partial^2 f_3}{\partial x_5 \partial x_3} = -\gamma_1 \frac{\beta_P}{N}, \quad \frac{\partial^2 f_5}{\partial x_2 \partial x_5} = \frac{\partial^2 f_5}{\partial x_5 \partial x_2} = -\gamma_2 \frac{\beta_D \alpha_D}{N},$$
$$\frac{\partial^2 f_5}{\partial x_3 \partial x_5} = \frac{\partial^2 f_5}{\partial x_5 \partial x_3} = -\gamma_2 \frac{\beta_D}{N}.$$

$$= \nu_2\Big(\frac{\partial^2 f_2}{\partial x_1 \partial x_3} + \frac{\partial^2 f_2}{\partial x_3 \partial x_1}\Big) + \nu_4\Big(\frac{\partial^2 f_4}{\partial x_1 \partial x_5} + \frac{\partial^2 f_4}{\partial x_5 \partial x_1}\Big) + \nu_3\Big(\frac{\partial^2 f_3}{\partial x_3 \partial x_5} + \frac{\partial^2 f_3}{\partial x_5 \partial x_3}\Big) +$$
$$\nu_5\Big(\frac{\partial^2 f_5}{\partial x_3 \partial x_5} + \frac{\partial^2 f_5}{\partial x_5 \partial x_3}\Big) + \nu_6\Big(\frac{\partial^2 f_6}{\partial x_1 \partial x_6} + \frac{\partial^2 f_6}{\partial x_6 \partial x_1}\Big)$$
$$= -\nu_2\Big(\psi_1\psi_2\frac{\beta_D}{N} + \psi_2\psi_1\frac{\beta_D}{N}\Big) - \nu_4\Big(\psi_1\psi_5\frac{\beta_P}{N} + \psi_5\psi_1\frac{\beta_P}{N}\Big) - \nu_3\gamma_1\Big(\psi_3\psi_5\frac{\beta_P}{N} + \psi_5\psi_3\frac{\beta_P}{N}\Big) -$$
$$\nu_5\gamma_2\Big(\psi_3\psi_5\frac{\beta_D}{N} + \psi_5\psi_3\frac{\beta_D}{N}\Big) - \nu_6\Big(\psi_1\psi_6\frac{\beta_{DP}}{N} + \psi_6\psi_1\frac{\beta_{DP}}{N}\Big)$$

Substituting ψ yields

$$= -2\frac{\beta_D}{N}\nu_2\psi_1\psi_2 - 2\frac{\beta_P}{N}\nu_4\psi_5\psi_1 - 2\frac{\beta_P}{N}\nu_3\gamma_1\psi_3\psi_5 - 2\frac{\beta_D}{N}\nu_5\gamma_2\psi_3\psi_5 - 2\frac{\beta_{DP}}{N}\nu_6\psi_1\psi_6$$
$$a = 2\frac{\beta_D}{\mu N}\psi_2\psi_3\nu_2\Big(\beta_D(\alpha_D\psi_2 + \psi_3) + \beta_P(\alpha_P\psi_4 + \psi_5)\Big) - 2\frac{\phi_D\beta_P}{k_4\mu N}\nu_4\psi_4\Big(\beta_D(\alpha_D\psi_2 + \psi_3) + \beta_P(\alpha_P\psi_4 + \psi_5)\Big) \tag{8}$$

$$b = \sum_{i,j,k=1}^{n} \nu_i\psi_j\frac{\partial^2 f_i}{\partial x_j \partial \beta_D^*}(x_0, \beta_D^*) \quad = \nu_2\frac{\partial^2 f_2}{\partial x_1 \partial \beta_D^*} \quad = \nu_2(\alpha_D\psi_2 + \psi_3) > 0 \tag{9}$$

In accordance with theorem 4.1 of [28], based on the coefficients of a and b, the systems of equation (7) will undergo backward bifurcation.

3.3.4 Sensitivity analysis of the reproductive number

In this subsection, the normalized forward sensitivity index of R_0 will be used to pinpoint the strength and weakness of each parameter in the models prediction. Therefore, The Normalized forward sensitivity index of R_0 differentiable with respect to a given parameter β defined as [29]

$$\Upsilon_{\beta_D}^{R_0} = \frac{\beta}{R_0}\frac{\partial R_0}{\partial \beta_D}$$

where

$$R_0 = \frac{b(1-V)(\beta_D(\alpha_D(\theta + \eta_D + \varpi_D + \mu) + \phi_D))}{\mu(\phi_D + \xi_D + \mu)(\theta + \eta_D + \varpi_D + \mu)}$$

Manual calculation of the sensitivity to parameter β_D

$$\frac{\beta_D}{R_0} = \beta_D\frac{\mu(\phi_D + \xi_D + \mu)(\theta + \eta_D + \varpi_D + \mu)}{b(1-V)(\beta_D(\alpha_D(\theta + \eta_D + \varpi_D + \mu) + \phi_D))}$$

$$\frac{\partial R_0}{\partial \beta_D} = \frac{b(1-V)(\alpha_D(\theta + \eta_D + \varpi_D + \mu) + \phi_D)}{\mu(\phi_D + \xi_D + \mu)(\theta + \eta_D + \varpi_D + \mu)}$$

By substituting the values of the epidemiological parameters to the above equations will manually compute the sensitivity of β_D, other parameters can be calculated.

4 Numerical Simulations

In this section, Numerical simulation for diphtheria and pertussis co-infection model is performed, The dynamics of the various compartments in the population was observed. Firstly, The epidemiology parameters in Table 1 was substituted into the three terms of reproduction number derived. The Figure 2, Figure 3 and Figure 4 shows the effect of vaccination V and corresponding contact rates of Diphtheria β_D, Pertussis β_P and diphtheria-pertussis β_{DP} with contour plots respectively.

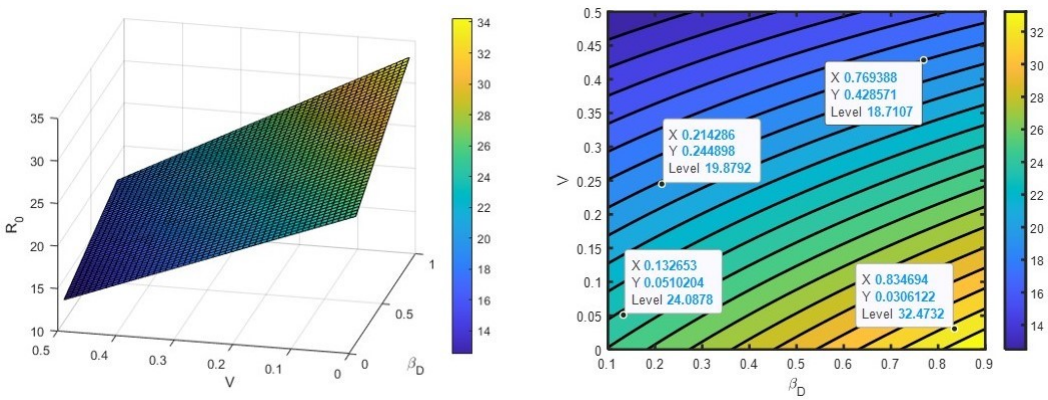

Figure 2: Effect of vaccination V and contact rate of diphtheria β_D on R_0 with contour plot.

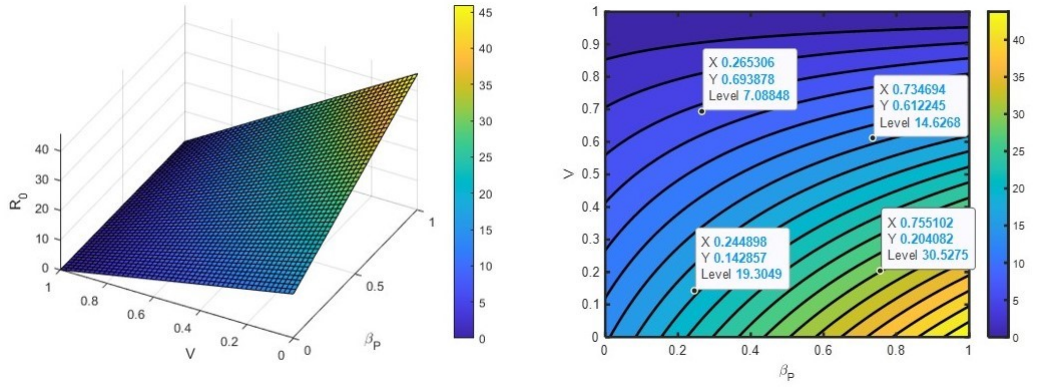

Figure 3: Effect of vaccination V and contact rate of pertussis β_P on R_0 with contour plot.

Furthermore, each parameter sensitivity in reproduction number was examined by varying the vaccination at birth V and quarantine of diphtheria θ as illustrated in the sensitivity bar chart Figure 6, Figure 7, Figure 8 and Figure 9. In Figure 8 We observed that When $V = 0.01$, and quarantine of individuals infected with diphtheria $\theta = 0$ arranging the parameter as regards its magnitude in descending order is $b = 1.0$, $\varpi_D = 0.59155$, $V = 0.5263$, $\beta_P = 0.414355$, $\beta_D = 0.363102$, $\beta_{DP} = 0.3150$, $\phi_P = 0.2524$, $\varpi_P = -0.206208$, $\xi_P = 0.191831$, $\xi_D = 0.168103$, $\eta_P = 0.167155$, $\phi_D = 0.139104$, $\eta_D = -0.0903332$, $\alpha_D = 0.0318801$, $\alpha_P = 0.027965$, $\varpi_D = -0.0215079$

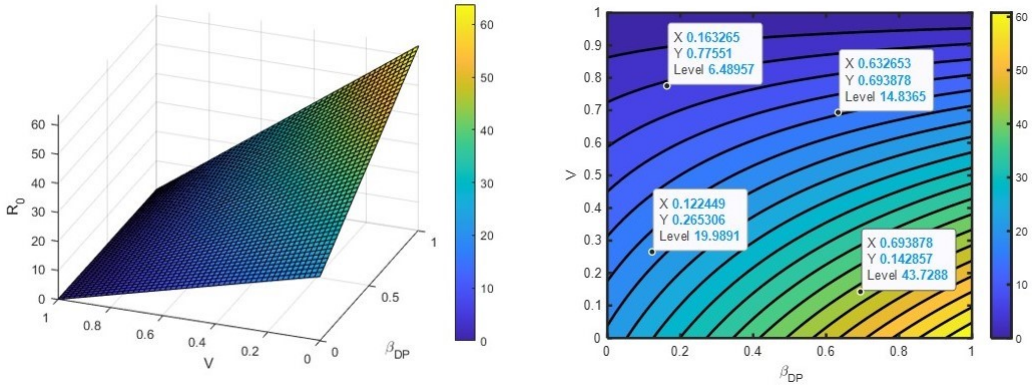

Figure 4: Effect of vaccination V and contact rate of pertussis β_{DP} on R_0 with contour plot.

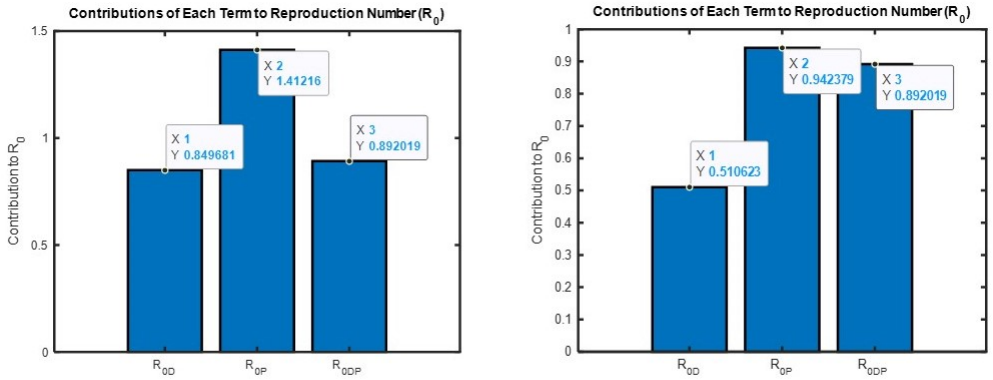

(e) V = 0.9, $\xi_D = \xi_P = 2$ (f) V = 0.9, $\xi_D = \xi_P = 3$

Figure 5: Bar chart showing Effect of Vaccination at Birth V with improved Maternally derived immunity on the three terms of R_0.

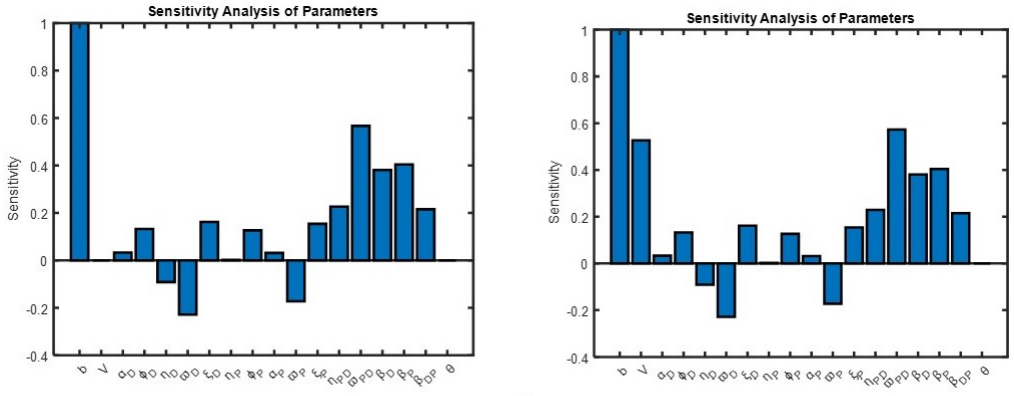

(a) V = θ = 0 (b) V = 0.01, θ = 0

Figure 6: Bar chart showing Effect of Vaccination at Birth V with improved Maternally derived immunity on the three terms of R_0.

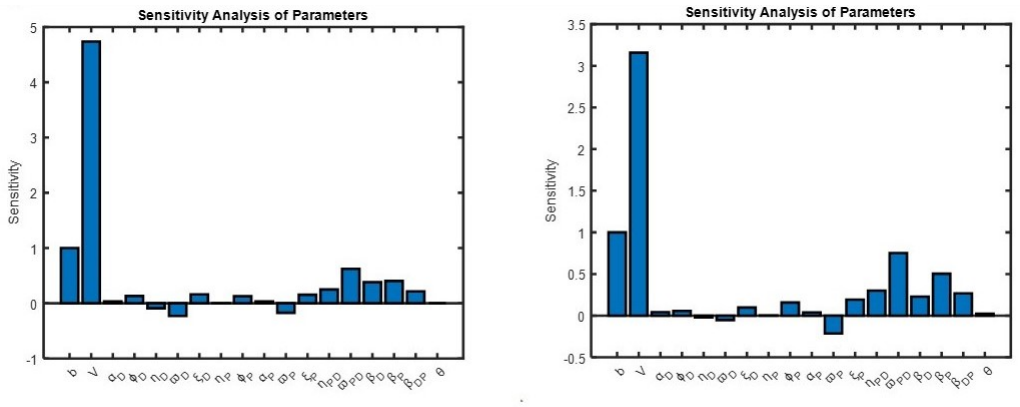

(c) V = 0.09, θ = 0 (d) V = 0.06, θ = 0.1

Figure 7: Impact of parameters on R_0 with vaccination and zero partial quarantine of diphtheria-pertussis model.

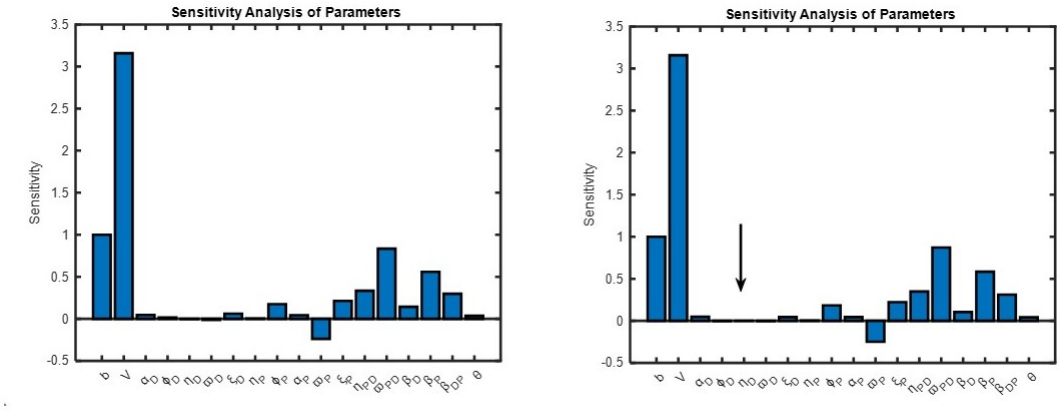

(e) V = 0.06, θ =0.3 (f) V = 0.06, θ = 0.6

Figure 8: Impact of parameters on R_0 with vaccination and partial quarantine of diphtheria.

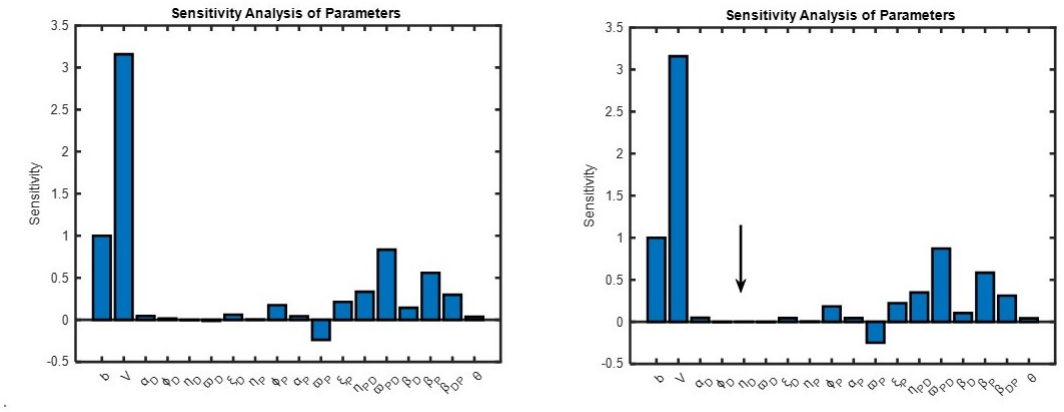

(e) V = 0.06, θ =0.3 (f) V = 0.06, θ = 0.6

Figure 9: Impact of improved vaccination, partial quarantine and maternal derived immunity parameters on R_0.

In the quest to obtain the best disease mitigating parameter for the non-optimal control strategy, a combination of disease controller was explored by varying there values in $(S, I_{AD}, I_{SD}, I_{AP}, I_{SP}, I_{SDP}, Q_{SD}, R)$

model. The initial size of the total population at time $t = 0$ day was $N(0) = 1000$, $S(0) = 900$, $I_{AD0} = 10$, $I_{SD0} = 5$, $I_{AP0} = 15$, $I_{SP0} = 20$, $I_{SDP0} = 25$, $Q = 0$, and $R = 20$ that is $(900, 10, 5, 15, 20, 25, 0, 20)$. The graphical experiment performed on the model dynamics at the initial instance of outbreak using table parameter without disease controller in Figure 10 shows that after $t = 100$ days the model reads $(176, 29, 103, 10, 44, 19, 0, 211)$. The model was also examined by increasing vaccination at birth, Figure 10 and Figure 11 indicates that when $V = 0.6$ and $\xi_D = \xi_P = \theta = 0$ the model compartments is approximately $(120, 12, 52, 0, 18, 4, 0, 992)$ after 100 days, . At a high vaccination administration $V = 0.9$, the model compartments approximately reads $(63, 0, 14, 0, 3, 0, 0, 1374)$.

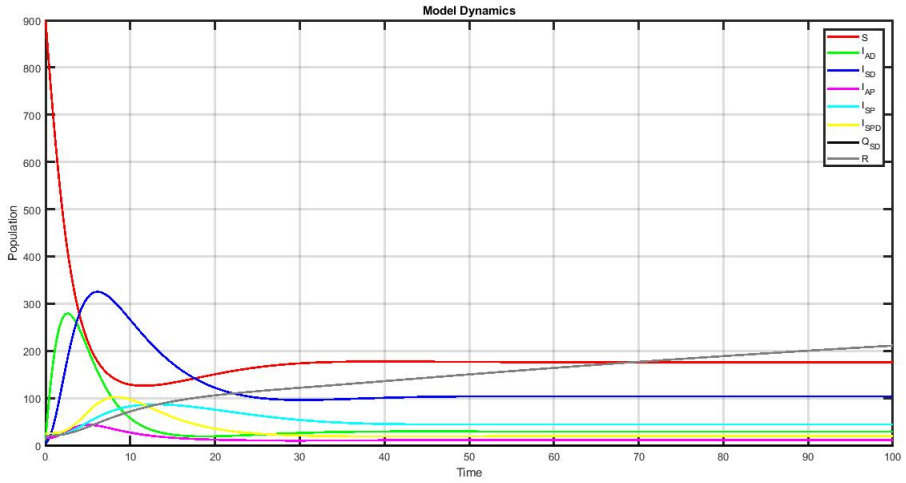

Figure 10: Zero Vaccination on $(S, I_{AD}, I_{SD}, I_{AP}, I_{SP}, I_{SDP}, Q_{SD}, R)$ Model.

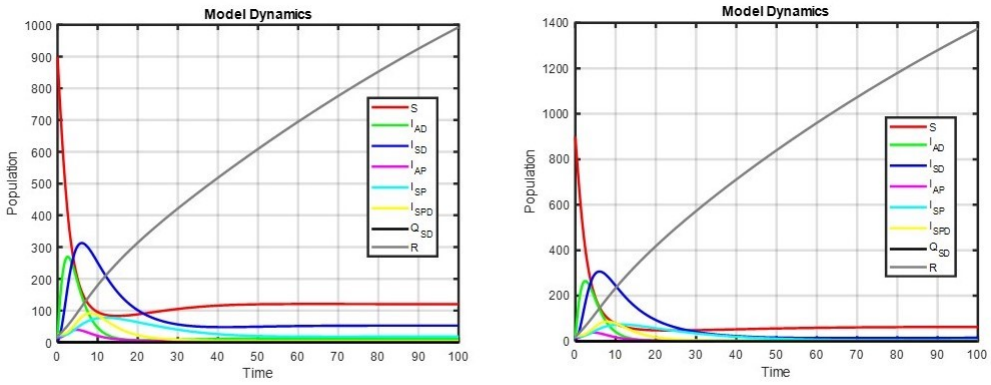

(c) V = 0.6, $\xi_D = \xi_P = \theta = 0$ (d) V = 0.9, $\xi_D = \xi_P = \theta = 0$

Figure 11: Varying Vaccination impact on $(S, I_{AD}, I_{SD}, I_{AP}, I_{SP}, I_{SDP}, Q_{SD}, R)$ Model.

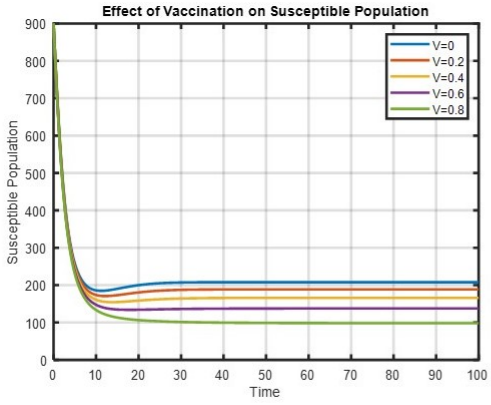

(a) varying vaccine effectiveness on S

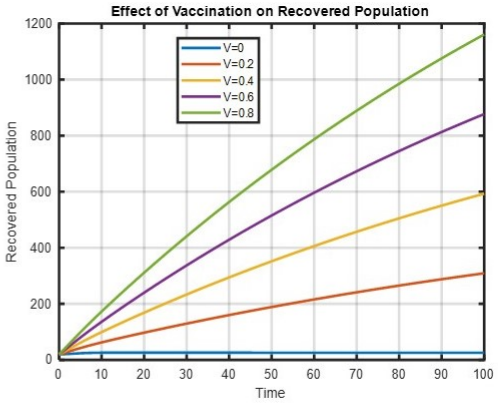

(b) varying vaccine effectiveness on R

Figure 12: Varying Vaccination effect on Susceptible and Recovered compartment.

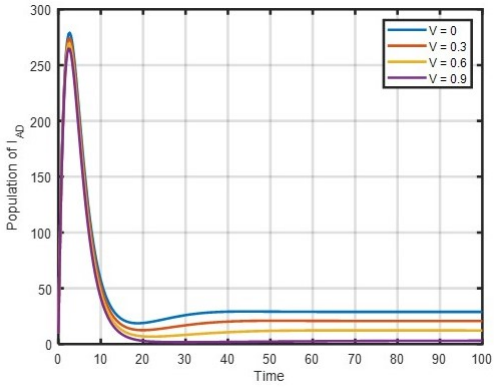

(c) varying vaccine effectiveness on I_{AD}

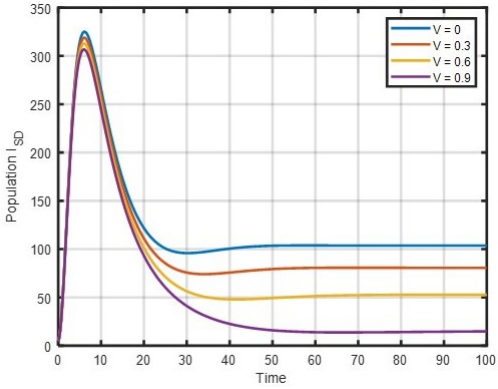

(d) varying vaccine effectiveness on I_{SD}

Figure 13: Varying Vaccination effect on Symptomatic and Asymptomatic infectious individuals with Diphtheria.

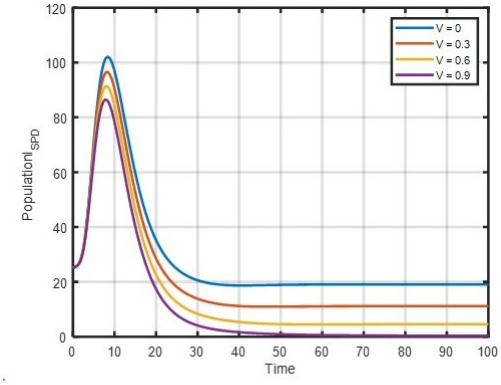

(e) Partial varying vaccine effectiveness on I_{SDP}

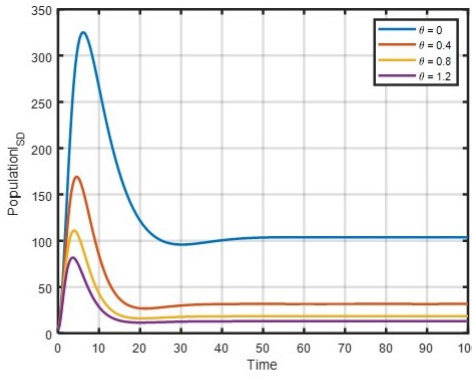

(f) varying quarantine effectiveness on I_{SD}

Figure 14: Varying Vaccination on symptomatically infected with diphtheria-pertussis and varying quarantine effect on Symptomatic infectious individuals with Diphtheria.

5 Discussion of results and conclusion

The theoretical results suggest that the $(S, I_{AD}, I_{SD}, I_{AP}, I_{SP}, I_{SDP}, Q_{SD}, R)$ model is both epidemiological and mathematically well-posed. The 3D graphical and contour plots show that increasing vaccination reduces the value of R_0. Furthermore, to emphasize the effectiveness of disease control measures, a bar chart was used to assess the impact of control reinforcement strategies. The findings indicate that combining control measures significantly reduces R_0.

A sensitivity analysis was conducted to identify the most influential parameter in R_0. When $V = 0.06$ and $\theta = 0.6$, the parameters arranged in descending order of influence are: V, ϖ_D, b, θ, β_P, ξ_P, ϕ_P, η_{DP}, β_{DP}, β_D, ξ_D, α_D, θ, α_P, η_P, ϕ_D, η_D, ϖ_D, ϖ_P. Additionally, the impact of disease control measures on each compartment in the model demonstrates that increasing vaccination rates significantly mitigates disease spread.

The model also shows backward bifurcation under certain conditions, Therefore, optimal control strategies should be explored in future research to effectively reduce multiple stable equilibria and control the disease dynamics.

References

[1] Khatiwada, A. P., Shrestha, N., and Shrestha, S. (2021). Will COVID-19 lead to a resurgence of vaccine-preventable diseases?.Infection and Drug Resistance, 119-124.

[2] Agüero, M. L., Castillo, J. B. D., Falleiros-Arlant, L. H., Berezín, E., de Moraes, J. C., Torres-Martínez, C., ... and López-Medina, E. (2023). Risks of low vaccination coverage and strategies to prevent the resurgence of vaccine-preventable diseases in infants in the COVID-19 pandemic scenario: recommendations for Latin America and the Caribbean by the group of experts on infant immunization for Latin America. Expert Review of Vaccines, 22(1), 1091-1101.

[3] Organization, W.H.: COVID-19 Pandemic Fuels Largest Continued Backslide in Vaccinations in Three Decades, https://www.who.int/news/item/15-07-2022- covid-19-pandemic-fuels-largest-continued-backslide-in-vaccinations-in-three decades. Accessed: 2024-05-26 (2022).

[4] Gouveia, N., and Fletcher, T. (2000). Respiratory diseases in children and outdoor air pollution in Sao Paulo, Brazil: a time series analysis. Occupational and environmental medicine, 57(7), 477-483.

[5] Clay, P. A., Duffy, M. A., and Rudolf, V. H. (2020). Within-host priority effects and epidemic timing determine outbreak severity in co-infected populations. Proceedings of the Royal Society B, 287(1922), 20200046.

[6] Cox, F. E. G. (2001). Concomitant infections, parasites and immune responses. Parasitology, 122(S1), S23-S38.

[7] Glidden, Caroline K., Courtney AC Coon, Brianna R. Beechler, Chase McNulty, Vanessa O. Ezenwa, and Anna E. Jolles. "Co-infection best predicts respiratory viral infection in a wild host." Journal of Animal Ecology 90, no. 3 (2021): 602-614.

[8] Griffiths, E. C., Pedersen, A. B., Fenton, A., and Petchey, O. L. (2011). The nature and consequences of coinfection in humans. Journal of Infection, 63(3), 200-206.

[9] Liang, J. L. (2018). Prevention of pertussis, tetanus, and diphtheria with vaccines in the United States: recommendations of the Advisory Committee on Immunization Practices (ACIP). Recommendations and reports, 67.

[10] Murphy, T. V., Slade, B. A., Broder, K. R., Kretsinger, K., Tiwari, T., Joyce, M. P., ... and Moran, J. S. (2008). Prevention of pertussis, tetanus, and diphtheria among pregnant and postpartum women and their infants. Recomm Rep, 57,1-51.

[11] Kuchar, E., Karlikowska-Skwarnik, M., Han, S., and Nitsch-Osuch, A. (2016). Pertussis: history of the disease and current prevention failure. Pulmonary dysfunction and disease, 77-82.

[12] Sadoh, A. E., and Oladokun, R. E. (2012). Re-emergence of diphtheria and pertussis: implications for Nigeria.Vaccine, 30(50), 7221-7228.

[13] Calderón, T. A., Coffin, S. E., and Sammons, J. S. (2015). Preventing the spread of pertussis in pediatric healthcare settings. Journal of the Pediatric Infectious Diseases Society, 4(3), 252-259.

[14] Brooks, D. A., and Clover, R. (2006). Pertussis infection in the United States: role for vaccination of adolescents and adults. The Journal of the American Board of Family Medicine, 19(6), 603-611.

[15] Yakubu, A. A., Abdullah, F. A., and Yatim, Y. M. (2022). Mathematical Model of Pertussis and Pneumonia Co-Infection in Infants with Maternally Derived Immunity. Sains Malaysiana, 51(7), 2197-2209.

[16] Teklu, S. W., and Mekonnen, T. T. (2021). HIV/AIDS-Pneumonia Coinfection Model with Treatment at Each Infection Stage: Mathematical Analysis and Numerical Simulation. Journal of Applied Mathematics, 2021(1), 5444605.

[17] Pérez, A. G. C., and Oluyori, D. A. (2022). A model for COVID-19 and bacterial pneumonia coinfection with community-and hospital-acquired infections. Mathematical Modelling and Numerical Simulation with Applications, 2(4), 197-210.

[18] Tilahun, G. T. (2019). Optimal control analysis of pneumonia and meningitis coinfection. Computational and Mathematical Methods in Medicine, 2019(1), 2658971.

[19] Omame, A., and Abbas, M. (2023). Modeling SARS-CoV-2 and HBV co-dynamics with optimal control. Physica A: Statistical Mechanics and its Applications, 615, 128607.

[20] Johnson, O. S., Edogbanya, H. O., Emmanuel, J., and Olukanni, S. E. (2023). Stability Analysis of COVID-19 Model with Quarantine. International Journal of Mathematical Sciences and Computing, 9(3), 26-45.

[21] Deressa, C.T., Mussa, Y. O., and Duressa, G. F. (2020). Optimal control and sensitivity analysis for transmission dynamics of Coronavirus. Results in Physics, 19, 103642.

[22] Kanchanarat, S., Chinviriyasit, S., and Chinviriyasit, W. (2022). Mathematical assessment of the impact of the imperfect vaccination on diphtheria transmission dynamics. Symmetry, 14(10), 2000.

[23] Izzati, N., and Andriani, A. (2021, April). Dynamical analysis of diphtheria epidemic model with natural immunity rate on exposed individuals. In Journal of Physics: Conference Series (Vol. 1869, No. 1, p. 012117). IOP Publishing.

[24] Burrell, C. J., Howard, C. R., and Murphy, F. A. (2016). Fenner and White's medical virology. Academic Press.

[25] Diekmann, O., Heesterbeek, J. A. P., and Metz, J. A. J. (1990). On the definition and the computation of the basic reproduction ratio R 0 in models for infectious diseases in heterogeneous populations. Journal of mathematical biology, 28, 365-382.

[26] Siddik, S. B. M., Abdullah, F. A., and Ismail, A. I. M. (2020). Mathematical Model of Dengue Virus with Predator-Prey Interactions. Malaysiana, 49(5), 1191-1200.

[27] Vargas-De-León, C. (2009). Constructions of Lyapunov functions for classic SIS, SIR and SIRS epidemic models with variable population size. Foro-Red-Mat: Revista electrónica de contenido matemático, 26(5), 1-12.

[28] Castillo-Chavez, C., and Song, B. (2004). Dynamical models of tuberculosis and their applications. Mathematical Biosciences amd Engineering, 1(2), 361-404.

[29] Johnson, O. S., Edogbanya, H. O., Wakili, A., and John, A. T. (2024). Diphtheria Disease Transmission Dynamics In Low Vaccine Coverage Setting. International Journal of Mathematical Sciences and Optimization: Theory and Applications, 10(2), 79-106.

[30] Edogbanya, H. O., Oladipupo, J. (2024). Mathematical Modeling for Mitigating Pertussis Resurgence in the Post-COVID-19 Era: A Sensitivity Analysis and Intervention Strategies.Federal University Lokoja. DOI: 10.5281/zenodo.10721146